www.lajss.org
Latin American Journal of Solids and Structures 3 (2006) 75–87

# Damage models and identification procedures for crashworthiness of automotive light materials

B. Bennani and F. Lauro*

Laboratoire d'Automatique, de Mécanique et d'Informatique industrielles et Humaines, Université de Valenciennes, UMR CNRS 8530, F-59313 Valenciennes Cedex 09, France.

Abstract

In order to improve predictions of crashworthiness of automotive light materials in finite element simulation, the ability of the explicit finite element codes to take complex failure into account has to be increased. In consequence, damage models based on the framework of continuum mechanics are presented. The first one focusses on the development of ellipsoidal microvoids during plastic strain, and the second one uses a global damage variable which evolves with the strain energy density release rate. An original damage parameters identification procedure based on an inverse technique with static and dynamic tests is used. The previous damage framework is applied to magnesium, aluminium and high strength steel materials.

## 1 Introduction

Crashworthiness simulation has been a major factor in enabling automotive manufacturers to achieve a 30 to 50% reduction in development time and costs over the past five years.

However, demand for greater weight savings and crashworthiness protection has only been possible using new design concepts and use of lightweight materials that have limited ductility and a complex failure. The possibility of failure is consequently a reality which could dramatically change the course of deformation events. The present crashworthiness codes are inadequate to predict failure in such materials, or jointing systems, which has raised serious uncertainties over their results. In order to avoid a return to a 'prototype based design' and to maintain the high level of safety achieved in recent years there is an urgent need to improve the failure prediction capabilities of crashworthiness simulation codes.

Consequently, it has been necessary to undertake a dedicated European research project called IMPACT [10] to develop models and methodologies for failure prediction. The results presented in this paper concern only the metallic materials like aluminium and magnesium which present complex failures under dynamic loadings. So, specific damage models based on the framework of continuum damage mechanics are used to describe the development of damage under mechanical loadings, its progression up to the initiation of a macro-crack and finally the

*Corresp. author Email: flauro@univ-valenciennes.fr Received 1 June 2005; In revised form 24 November 2005

growth of this macro-crack up to failure of the component. A damage model such as Gologanu's model which could describe all these phenomenon by introducing an accurate description of the evolution of the microvoids under dynamic loadings is therefore used. The shape and orientation of the microstructural cavities are taken into account in the finite element model developed so as to improve prediction of damage and fracture occurrence. The growth, nucleation and coalescence phases are considered to describe the evolution of the microvoid volume fraction. The evolution law of porosity due to nucleation is modified to take damage evolution during pure shear loading into account.

A macroscopic approach, less expensive in terms of number of parameters to identify, and based on Lemaitre's model is also used to check its ability to represent correctly the damage evolution under dynamic loadings. Lemaitre's model for ductile damage was established for isotropic conditions and later on extended to include the possibility of anisotropy in the development of damage. The damage law is used either in monotonic loadings for the ductile fracture or in cyclic loadings for low cycle or high cycle loadings. This damage law depends on the strain energy density release rate which is the principal variable which governs the phenomenon of damage.

As the damage evolution is localised in the large plastic strain zone, the evolution damage law and threshold parameters must be identified in this zone. An original approach based on an inverse method is used. This method consists in the identification of the damage parameters by correlating an experimental and numerical macroscopic measurement strongly dependent on the parameters. Dynamic tensile tests on thin notched specimens are used as mechanical tests to measure macroscopic responses. The experimental data obtained is the variation of the inner radius of the specimens according to their elongation as well as the variation of forces according to the elongation of the specimens. Previous damage models are applied to simulate specimens and parts for aluminium, magnesium and high stress steel materials. Their ability to predict the stress softening, the damage and the failure path are illustrated and the results are discussed.

## 2 Constitutive models and parameters identification procedures

### 2.1 Damage models

#### 2.1.1 Gologanu's model

The Gologanu, Leblond and Devaux model (GLD) extends the Gurson, Tvergaard and Needleman model (GTN) to take the microvoid shape effect into account [1, 7–9, 11, 12]. The GLD model is based on the analysis of an ellipsoidal cavity embedded in a medium which has the shape of a confocal.

Due to the shape of the microvoid and its evolution, anisotropy of the damage is then introduced. The microvoid can also change in direction following the loading direction which in turn could then change the direction of the crack propagation.

The plastic potential takes the following form:

$$\phi_{evp} = \mathbf{C}\,\frac{\left\|\boldsymbol{\sigma}' + \eta\ \sigma_H\ \mathbf{X}\right\|^2}{\sigma_M^2} - \varphi = 0 \tag{1}$$

where

$$\varphi = 1 + \left(q_1\ f^*\right)^2 - 2\ q_1\ f^*\ \cosh\left(\upsilon\right) \quad ,\upsilon = \frac{\kappa\ \sigma_H}{\sigma_M} \quad ,\sigma_H = \left(1 - 2\ \alpha_2\right)\ \sigma_{11} + \alpha_1\ \sigma_{22} \tag{2}$$

The notation $\|\bullet\|$ is used in the original GLD potential to express the calculation of the von Mises norm $\left(\|\mathbf{T_{ij}}\| = [1.5\mathbf{T_{ij}}\mathbf{T_{ij}}]^2\right)$ applied to the deviator stress $\boldsymbol{\sigma}'$on which $\eta\,\sigma_H\,\mathbf{X}$ product is added. The material anisotropy is introduced with the Hill 48 norm. The parameters $\eta, \alpha_1, \alpha_2, \mathbf{X}, \mathbf{C}$ are functions depending on the porosity and the shape parameter S is defined by the evolution law:

$$\begin{aligned}\dot{S} =& \frac{3}{2}\left(1 + \frac{9}{2}h_T(T,\zeta)(1-\sqrt{f})^2\frac{\alpha_1 - \alpha_1^G}{1 - 3\alpha_1}\right)\left(\dot{\varepsilon_{11}} - \frac{\dot{\varepsilon_{kk}}}{3}\right) + \\ &+ \left(\frac{1 - 3\alpha_1}{f} + 3\alpha_2 - 1\right)\dot{\varepsilon_{kk}}\end{aligned} \tag{3}$$

in which $h_T\left(T,\zeta\right)$ dependent on the triaxiality $T \equiv \sigma_{kk}\,/\,(3\ \sigma_{eq})$ according to the sign of $\zeta = \sigma_{kk}\ {\sigma'}_{ii}$, is given by:

$$\begin{cases} h_T\left(T,\zeta\right) = 1 - T^2 & for \quad \varsigma \geq 0 \\ h_T\left(T,\zeta\right) = 1 - \frac{T^2}{2} & for \quad \varsigma < 0 \end{cases} . \tag{4}$$

and $\alpha_1$ and $\alpha_1^G$ are obtained by:

$$\alpha_1 = \frac{1}{2\,e_1^2} - \frac{1 - e_1^2}{2\,e_1^3}\ \tanh^{-1}\left(e_1\right) \tag{5}$$

$$\alpha_1^G = \frac{1}{3 - e_1^2} \tag{6}$$

with $e_1$ the main axis of the frame of the void.

The microvoid volume fraction is defined by

$$f = \frac{V_{voids}}{V_A} = 1 - \frac{V_M}{V_A}, \tag{7}$$

where $V_A$, $V_M$ are respectively the elementary apparent volume of the material and the corresponding volume of the matrix.

The evolution of the microvoid volume fraction is expressed by:

$$\dot{f} = \dot{f}_{growth} + \dot{f}_{nucleation} \tag{8}$$

where $\dot{f}_{growth}$ and $\dot{f}_{nucleation}$ are respectively, the growth and nucleation rate of microvoids.

The rate of increase of the microvoid volume fraction, due to the growth of existing microvoids is given by:

$$\dot{f}_{growth} = (1 - f)\ \dot{\varepsilon}_{kk} \tag{9}$$

where $\dot{\varepsilon}_{kk}$ is the first invariant of the plastic strain rate tensor. The nucleation microvoid volume fraction rate is divided in a part controlled by the equivalent plastic strain and a pure shear part and is finally expressed by:

$$\begin{aligned} \dot{f}_{nucleation} =& \frac{f_N}{S_N\sqrt{2\pi}} \exp\left\{-\frac{1}{2}\left(\frac{\varepsilon_M - \varepsilon_N}{S_N}\right)^2\right\}\dot{\varepsilon}_M + \\ &+ \frac{f_S}{S_S + \sqrt{2\pi}} \exp\left\{-\frac{1}{2}\left(\frac{\varepsilon_{xy} - \varepsilon_S}{S_S}\right)^2\right\}\dot{\varepsilon}_{xy} \end{aligned} \tag{10}$$

where $f_N$, $f_S$ are nucleated microvoid volume fractions, $S_N$, $S_S$ are Gaussian standard deviations, $\varepsilon_N$, $\varepsilon_S$ are mean effective plastic strains for nucleation, $\varepsilon_M$ is the effective plastic strain and $\varepsilon_{xy}$ is the shear strain.

The coalescence function is then defined in function of f by:

$$f^* = \begin{cases} f & if\ f \le f_c \\ f_c + \frac{1/q_1 - f_c}{f_F - f_c}\ (f - f_c) & if\ f > f_c \end{cases} \tag{11}$$

where $f_c$ is the critical microvoid volume fraction at coalescence onset and $f_F$ is the microvoid volume fraction when ductile fracture occurs. The material is then virgin for a coalescence function equal to zero and is fully voided when the coalescence function reaches the value of $1/q_1$ with no stiffness.

### 2.1.2 Lemaitre's model

The isotropic damage evolution is described by the scalar D, representing the surface density of intersections of microcracks and microcavities with any plane in the body [5, 6]. The damage scalar variable is defined as

$$D = \frac{A_{voids}}{A_A} = 1 - \frac{A_M}{A_A} \tag{12}$$

in which $A_{voids}$, $A_A$ and $A_M$ are the voids, apparent and matrix sectional areas for any normal n respectively.

The damage evolution during plastic straining is defined by the following expression:

$$\dot{D} = \left(\frac{Y}{S}\right)^s \dot{\varepsilon}^p \text{ if } \varepsilon^{\mathrm{p}} > \varepsilon_D \tag{13}$$

in which Y is the damaged strain energy rate, S and s are material coefficients, $\varepsilon^p$ is the effective plastic strain and $\varepsilon_D$ is the plastic strain at damage threshold.

The strain energy density release rate which governs the phenomenon of damage is expressed by:

$$Y = \frac{(1+\nu)}{2E\,(1-D)^2}\left\langle \boldsymbol{\sigma}_{\mathbf{ij}}\right\rangle \left\langle \boldsymbol{\sigma}_{\mathbf{ij}}\right\rangle - \frac{\nu}{2E\,(1-D)^2}\left\langle \sigma_{kk}\right\rangle^2 \tag{14}$$

in which $\langle\sigma\rangle = \sigma$ if $\sigma \geq 0$ and $\langle\sigma\rangle = 0$ if $\sigma < 0$, $\sigma_{ij}$ the Cauchy stress tensor, $\nu$ Poisson's ratio of elastic contraction and E Young's modulus of elasticity.

Lemaitre's damage model is based on the strain equivalence hypothesis which states that any strain constitutive equation for a damaged material may be derived in the same way as for a virgin material (D equals to zero) except that the Cauchy stress tensor $\sigma$ is replaced by a damaged stress tensor as follows:

$$\tilde{\boldsymbol{\sigma}} = \frac{\boldsymbol{\sigma}}{1-\mathrm{D}}. \tag{15}$$

The equivalent plastic stress is then expressed by:

$$\sigma_{eq}\left(\tilde{\boldsymbol{\sigma}}\right) = \left[\frac{3}{2}\left(\tilde{\boldsymbol{\sigma}}\right)\ \ [\mathbf{H}]\ \ \left(\tilde{\boldsymbol{\sigma}}\right)\right]^{1/2} = \left[\frac{3}{2}\left(\frac{\boldsymbol{\sigma}}{1-D}\right)\ \ [\mathbf{H}]\ \ \left(\frac{\boldsymbol{\sigma}}{1-D}\right)\right]^{1/2} \tag{16}$$

where $[\mathbf{H}]$ is Hill's behaviour tensor for anisotropic material description.

In the viscoplastic domain, the viscoplastic potential can be written as follows:

$$\Omega_{vp} = \sigma_{eq}\left(\tilde{\boldsymbol{\sigma}}\right) - \sigma_v\left(\varepsilon^p, \dot{\varepsilon}^p\right) \tag{17}$$

with $\sigma_v\left(\varepsilon^p, \dot{\varepsilon}^p\right)$ the viscous flow stress experimentally determined which controls the strain-rate sensitivity of the material.

## 2.2 Identification of the damage parameters

An identification method based on an inverse technique is used. This method consists in the identification of the damage parameters by correlating, with an optimisation process (Fig. 1), an experimental and numerical macroscopic measurement strongly dependent on the parameters [4]. Tensile tests of notched flat specimens with 2, 3 and 4 mm radii are used as experimental tests. The variation in the bottom of the notch in function of the elongation of the notched specimen and the variation of the axial force in function of the elongation of the notched specimen are used as macroscopic measurements. The finite element simulations of the tests are carried out with the exact boundaries conditions of the experimental set up. For strain rate sensitive materials like steel, the tensile tests are performed for different plastic strain rates, covering the range of crash tests (0 to 500 $\mathrm{s}^{-1}$) by using a quasi-static test machine, servohydraulic test machine and Hopkinson bar (Fig. 2) [2]. A high speed camera, laser extensometer and image analyser are used to measure the experimental macroscopic response. An imaging correlation program has been developed to obtain the experimental information in the case of dynamic loadings. The measurements previously defined are then calculated following the evolution of the shape of the specimen by means of a speed camera and in house software. For the Hopkinson bars only the strength versus elongation of the specimen is used due to the poor number of images obtained at high speed loadings.

Finally, the correlation is obtained by minimising a cost function which is defined by the least square approximation as:

$$Q(\alpha) = \sum_{i=1}^{nb\_point} \frac{\left[Z_i^{sim}(\alpha) - Z_i^{\exp}\right]^2}{\left[Z_i^{\exp}\right]^2} \tag{18}$$

where $\alpha$ are the material parameters to identify, $Z_i^{sim}$and$Z_i^{\exp}$ are the simulated and experimental macroscopic responses and nb_point is the number of experimental points of the experimental response.

The scalar material parameters are $\alpha$={$q_1$, f, $f_N$, $S_N$, $\varepsilon_N$, S, $f_c$, $f_F$} and $\alpha$={$\varepsilon_D$, $D_c$, S, s} in the case of GLD's model and Lemaître's model respectively. A first initial curve called "numerical non optimised" on figure 1 is obtained with the initial parameters and after some iterations becomes the "numerical optimised" with the optimised parameters.

The damage parameters of 6014 T7 aluminium alloy and Mg AM 50 magnesium are identified using the identification procedure presented (Tables 1 and 2). The aluminium material has a high ductility with a weak anisotropy in behaviour and damage due to the extrusion process. The magnesium material has a low ductility with a low damage evolution and can be considered as isotropic. In consequence, the critical damage $D_c$ is low for the Lemaitre model and the critical microvoid volume fraction at coalescence onset $f_c$ is also low considering the initial damage $f_0$ for the Gologanu model. For this latest model the nucleation works mainly at a very low equivalent plastic strain which quickly increases the damage value.

Table 1: Damage parameters of 6014 T7 aluminium alloy.

| | | | | | | | | |
|---|---|---|---|---|---|---|---|---|
| Gologanu's | $q_1$(-) | $S_0$(-) | $f_N$(-) | $S_N$(-) | $\varepsilon_N$(-) | $f_c$(-) | $f_F$(-) | $f_0$(-) |
| model | 1.52 | 0.001 | 0.040 | 0.1 | 0.19 | 0.06 | 0.08 | 0.001 |
| Lemaitre's | $\varepsilon_D$(-) | s(-) | S(MPa) | $D_c$(-) | | | | |
| model | 0.05 | 2 | 1.22 | 0.34 | | | | |

Table 2: Damage parameters of Mg AM 50 magnesium.

| | | | | | | | | |
|---|---|---|---|---|---|---|---|---|
| Gologanu's | $q_1$(-) | $S_0$(-) | $f_N$(-) | $S_N$(-) | $\varepsilon_N$(-) | $f_c$(-) | $f_F$(-) | $f_0$(-) |
| model | 1.98 | 0. | 0.0795 | 0.114 | 0.034 | 0.0385 | 0.043 | 0.001 |
| Lemaitre's | $\varepsilon_D$(-) | s(-) | S(MPa) | $D_c$(-) | | | | |
| model | 0. | 1.85 | 20 | 0.001 | | | | |

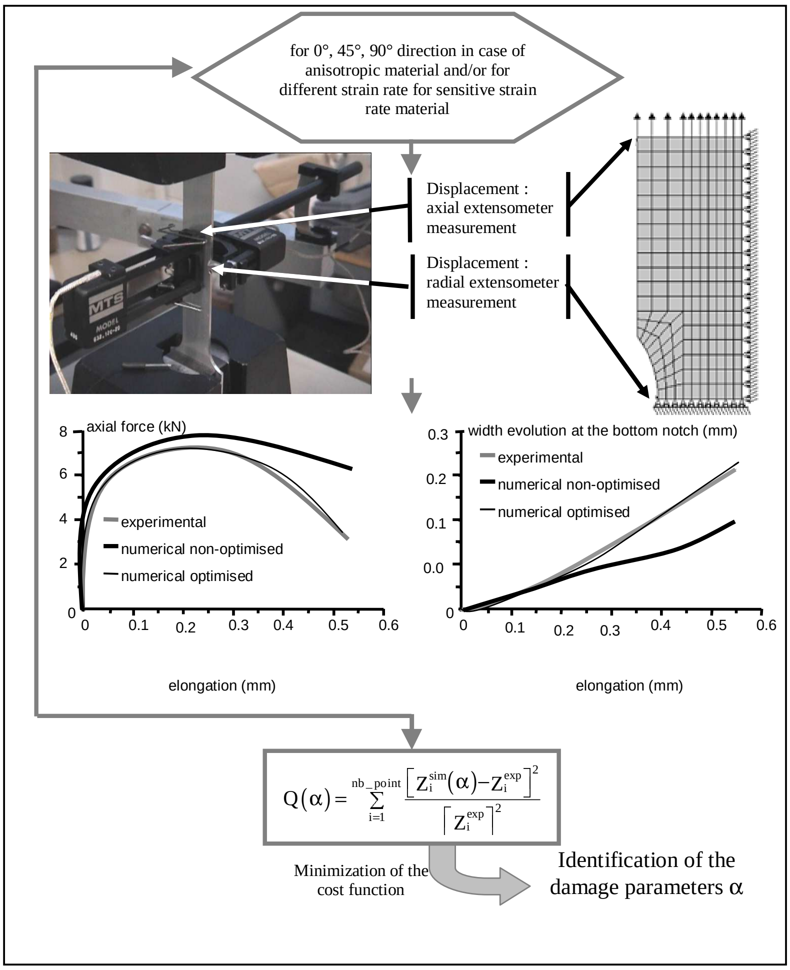


Figure 1: Inverse approach – Identification procedure to obtain damage parameters by correlating experimental and numerical measurements.

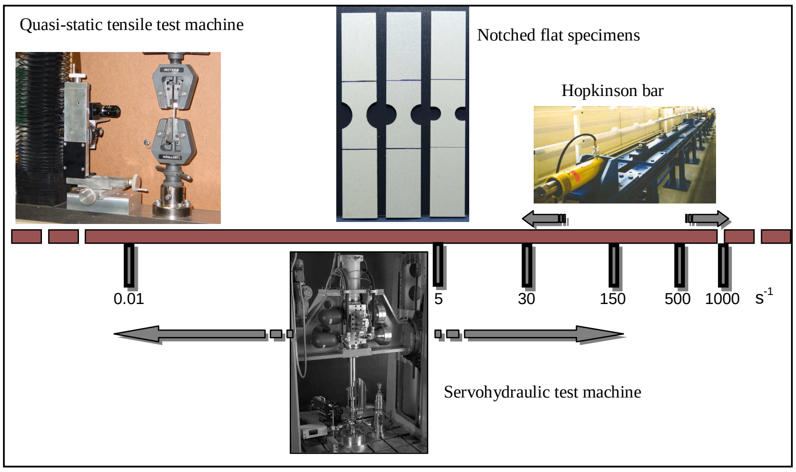


Figure 2: Tensile tests for different plastic strain rates using quasi-static, servohydraulic and Hopkinson bar test machines.

# 3 Applications

## 3.1 Magnesium material

### 3.1.1 Iosipescu test

Lemaitre's damage model is used to simulate the damage evolution of the magnesium specimen under pure quasi-static shear loading known as Iosipescu's test (Fig. 3) [3]. The damage parameters previously identified are used. The test is performed until fracture occurs with 5228 solid elements with height integration points and three elements through the thickness (thickness: 3,3mm). The contact between the rigid device and the specimen is assumed as perfect.

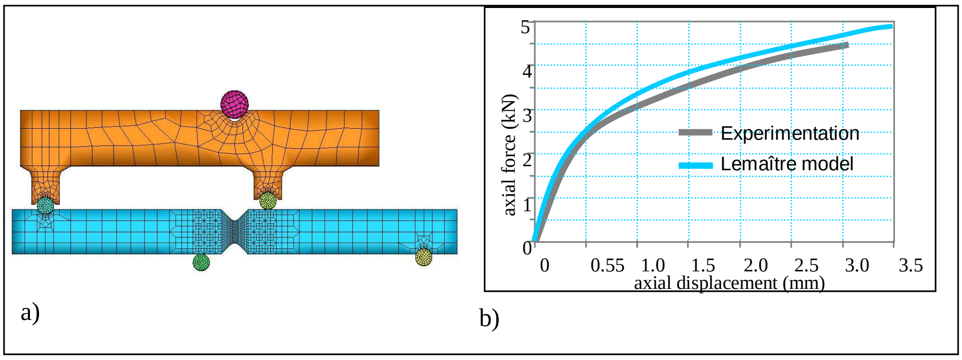


Figure 3: a) Finite element model of Iosipescu test and, b) experimental and numerical forces versus displacement

The Mg AM 50 magnesium is an isotropic material. The stress-strain relationship is identified (Fig. 4).

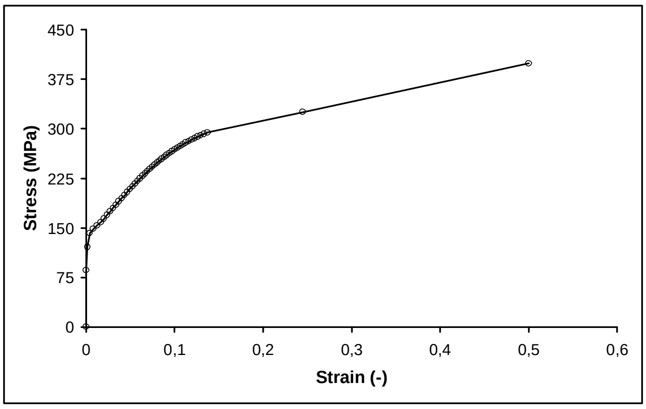


Figure 4: Behaviour law for Mg AM50 magnesium.

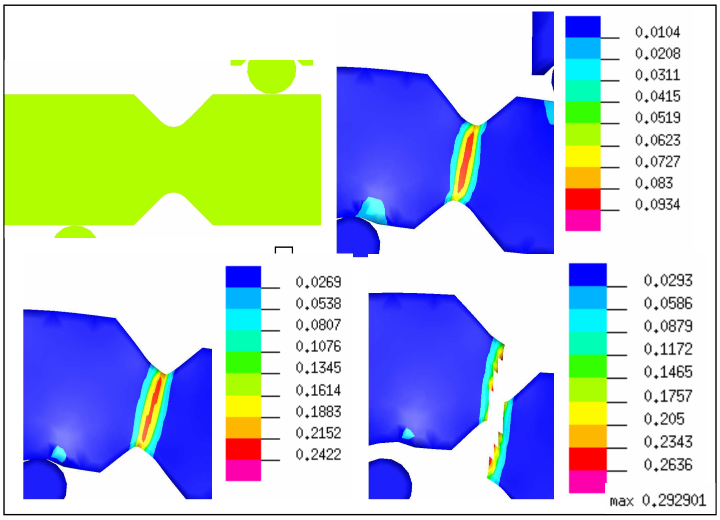


Figure 5: Plastic strain evolution in the finite element model of Iosipescu test.

The fracture due to pure shearing is correctly predicted by Lemaitre's model (Fig.5 and 6). The damage begins in the centre of the specimen and spreads from the centre to the edge of the notch. A thin band of damage characterizing the pure shear loading is then created, leading to the fracture of the specimen when a finite element reaches the critical value of damage Dc (Fig. 5).

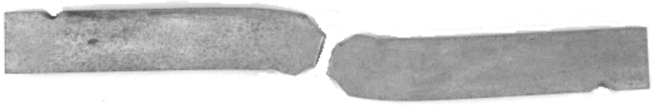

(a)

(b)

Figure 6: Comparison at the end of the test of the numerical and experimental shapes

### 3.2 Extruded tube

A dynamic test of an impact bending on a notched extruded tube is performed experimentally and numerically at 3 meters/second with 50 mm radius impactor of 275 kg mass. The numerical model consists of 15,614 shell elements (Fig. 4) with a minimum size element of 1mm. For the solid model the mesh is similar with three elements in the thickness. The failure is simulated by element elimination with both the Gologanu and Lemaitre damage models.

The 6014 T7 aluminium alloy is an orthotropic material. The corresponding HILL 48 material parameters are identified using 0$^\circ$, 45$^\circ$ and 90$^\circ$ tensile tests from the rolling directions (Table 3). The behaviour law in the 0$^\circ$ direction is given in figure 7.

Table 3: HILL 48 material parameters.

| F | G | L | M | N |
|---|---|---|---|---|
| 1.049 | 1.3 | 3 | 3 | 3.13 |

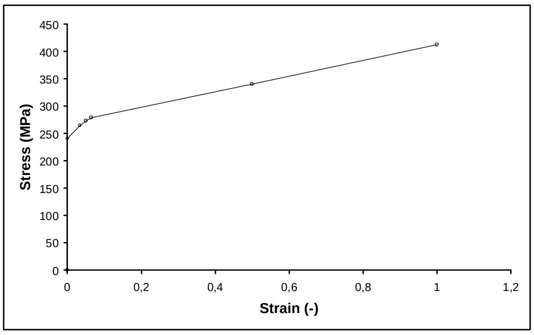


Figure 7: Behaviour law in the 0$^\circ$ direction for 6014 T7 aluminium alloy.

The experimental and numerical results are in good agreement in terms of instant of failure, failure path and energy dissipation in particular for Lemaitre's model (Fig. 8, Fig. 9). The Golaganu model with shell elements is accurate until the first element elimination but after that, the strain control of the damage leads to an underestimation of the energy dissipation along the failure.

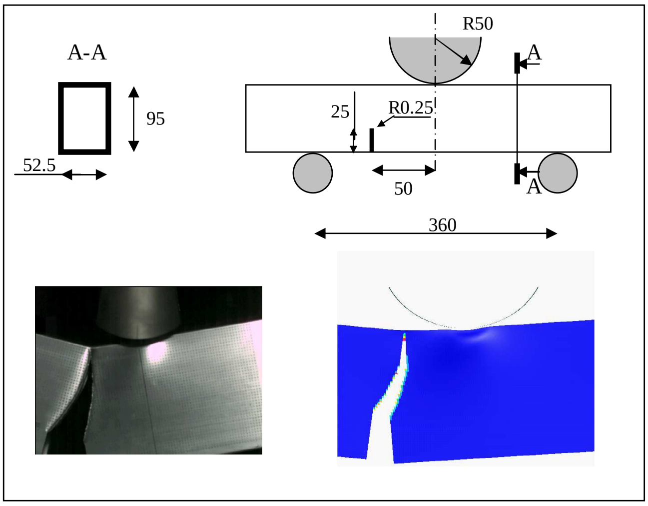


Figure 8: Finite element model of impact bending test.

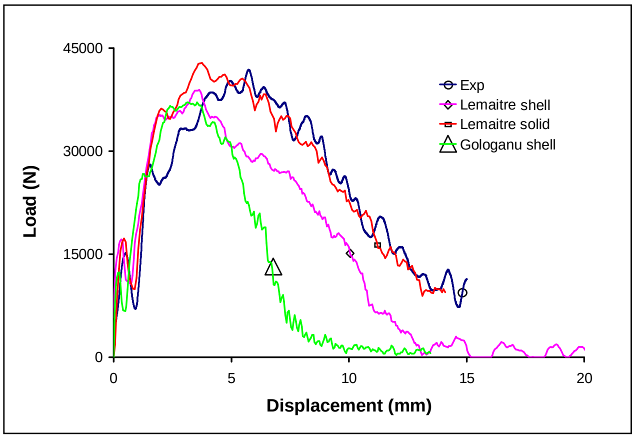


Figure 9: Experimental and numerical load versus displacement curves.

Nevertheless, when using shell elements, finite elements simulations lead to an underestimation of the dissipated energy which is explained by the fact that shell elements can not take the through thickness stresses into account even with seven integration points through the thickness as in these simulations. With solid elements the results are extremely promising.

## 4 Conclusions

In this paper, the Gologanu and Lemaitre damage models are presented. They have been modified by introducing the Hill potential to take anisotropy of the material into account. An inverse procedure using an optimizer to correlate experimental and numerical responses of notched specimen tensile tests is used to determine the damage parameters of both damage models. This procedure was applied to a magnesium part and an aluminium part and led to appropriate values of damage parameters in a convenient time for numerical simulations. These values come from an optimisation process which gives the best solution possible for a range of possibilities. The reality of these values can always be discussed but they are certainly close to the real ones.

An Iosipescu's test on a specific magnesium specimen and an impact bending test on a notched aluminium extruded tube to localize the failure were performed. The numerical computations were carried out using both damage models and the identified parameters. In general, the predicted energy dissipation and the failure instant and propagation were found to be in good agreement with the experimental measures. Nevertheless, as both identification procedures are still mesh dependent a regularisation technique should be used to avoid this dependency. Both damage models have a high level of accuracy and can be used for crash simulations. The Gologanu damage model is very accurate and the use of ellipsoidal microvoids allows one to have a damage anisotropic evolution which is very interesting for some materials. The complexity of this model is however a disadvantage for industrial applications. The Lemaitre damage model is easier to use and identify due to the small number of parameters. The stress control of the damage evolution is certainly an advantage in the simulation.

### Acknowledgements

The present research work is part of the Brite Euram Project IMPACT N° G3RT-CT-2000-00186.

The present research work has been supported by the CNRS, the European Community, the Conseil Régional Nord Pas de Calais, the Ministère de l'Education Nationale, the Délégation Régionale à la Recherche et à la Technologie; the authors gratefully acknowledge the support of these institutions.

### References

[1] P. Croix, F. Lauro, and J. Oudin. Anisotropic damage for aluminium. *International Journal of forming processes*, 5:269–285, 2002.

[2] O.S. Hopperstad, T. Borvik, M. Langseth, K. Labibes, and C. Albertini. On the influence of stress triaxiality and strain rate on the behaviour of a structural steel. part i : Experiments. *European Journal of Mechanics A/Solids*, 22:1–13, 2003.

[3] N. Iosipescu. New accurate procedure for single shear testing of metals. *Journal of Materials*, 2:537–566, 1967.

[4] F. Lauro, B. Bennani, P. Croix, and J. Oudin. Identification of the damage parameters for anisotropic materials by inverse technique: application to an aluminium. *Journal of Materials Processing Technology*, 118:472–477, 2001.

[5] J. Lemaitre. *A course of damage mechanics*. Springer-Verlag, 1989.

[6] J. Lemaitre, R. Desmorat, and M. Sauzay. Anisotropic damage law of evolution. *European. Journal of Mechanics A/Solids*, 19:187–208, 2000.

[7] A. L.Gurson. Continuum theory of ductile rupture by void nucleation and growth: Part i – yield criteria and flow rules for porous ductile media. *Engineering Material Technology*, 99:2–15, 1977.

[8] M.Gologanu, J.B.Leblond, and J. Devaux. Approximate models for ductile metals containing non-spherical voids – case of axisymmetric prolate ellipsoidal cavities. *Journal of the mechanics and physics of solids*, 41:1723–1754, 1993.

[9] M.Gologanu, J.B.Leblond, and J. Devaux. Numerical and theoretical study of coalescence of cavities in periodically voided solids. *Computational Material Modelling*, 42:223–244, 1994.

[10] Framework V project. Improved failure prediction for advanced crashworthiness of transportation vehicles. *G3RD-CT-2000-00186*, 2000-2003.

[11] V. Tvergaard. Influence of voids on shear band instabilities under plane strain conditions. *International Journal of fracture*, 17:389–407, 1981.

[12] V. Tvergaard. On localization in ductile materials containing spherical voids. *International Journal of fracture*, 18:237–252, 1982.